




Article

Development and Measurement of a Very Thick Aerodynamic Profile for Wind Turbine Blades

Alois Peter Schaffarczyk ^{1,*}, Brandon Arthur Lobo ^{1,†,‡}, Nicholas Balaesque ^{2,†}, Volker Kremer ^{3,†},
Janick Suhr ^{2,†} and Zhongxia Wang ^{1,§}

¹ Mechanical Engineering Department, Kiel University of Applied Sciences, D-24149 Kiel, Germany; lobobrandon@gmail.com (B.A.L.); zhongxia81@outlook.com (Z.W.)

² Deutsche WindGuard Engineering GmbH, D-27580 Bremerhaven, Germany; n.balaesque@windguard.de (N.B.); janick.suhr@windguard.de (J.S.)

³ AEROVIDE GmbH, 24768 Rendsburg, Germany; volker.kremer@aerovide.com

* Correspondence: alois.peter.schaffarczyk@fh-kiel.de or alois.schaffarczyk@fh-kiel.de; Tel.: +49-431-210-2610

† These authors contributed equally to this work.

‡ Current address: Industriestr. 2, D-70565 Stuttgart, Germany

§ Current address: Huijiyuanshequ 16-902, Beijing 100027, China

Abstract: We designed 60% thick airfoil to improve the aerodynamic performance in the root region of wind turbine rotor blades, taking into account current constraints. After an extensive literature review and patent research, a design methodology (including the considerations of simple manufacturing) was set up, and extensive 2D- and 3D-CFD investigations with four codes (Xfoil, MSES, ANSYS fluent, and DLR-tau) were performed, including implementation inside a generic 10 MW test-blade (CIG10MW). Comparison with results from Blade Element Momentum (BEM) methods and the estimation of 3D effects due to the rotating blade were undertaken. One specific shape (with a pronounced flat-back) was selected and tested in the Deutsche WindGuard aeroacoustic Wind Tunnel (DWAA), in Bremerhaven, Germany. A total of 34 polars were measured, included two trailing edge shapes and aerodynamic devices such as vortex generators, gurney flaps, zig-zag tape, and a splitter plate. Considerable changes in lift and drag characteristics were observed due to the use of aerodynamic add-ons. With the studies presented here, we believe we have closed an important technological gap.

Keywords: thick aerodynamic profile; wind turbine blade; CFD; wind-tunnel measurement



Citation: Schaffarczyk, A.P.; Lobo, B.A.; Balaesque, N.; Kremer, V.; Suhr, J.; Wang, Z. Development and Measurement of a Very Thick Aerodynamic Profile for Wind Turbine Blades. *Wind* **2024**, *4*, 190–207. <https://doi.org/10.3390/wind4030010>

Academic Editor: Francesco Castellani

Received: 11 April 2024

Revised: 14 June 2024

Accepted: 2 July 2024

Published: 12 July 2024



Copyright: © 2024 by the authors. Licensee MDPI, Basel, Switzerland. This article is an open access article distributed under the terms and conditions of the Creative Commons Attribution (CC BY) license (<https://creativecommons.org/licenses/by/4.0/>).

1. Introduction

1.1. State of the Art

Over the past three decades, advancements in wind energy technology have been substantial, largely attributed to the efforts of many scientists and companies. These advancements have resulted in significant reductions in specific electricity production costs, improved overall plant performance, and enhanced efficiency [1]. However, in order to further enhance energy conversion efficiency and due to the state of the art already achieved, it has become necessary to focus on optimizing rather minor details that were not previously seriously considered. One such detail is the transition area located around 20% of the relative rotor blade length, which encompasses the root region of the rotor blade.

Until now, the design of this particular area has primarily focused on meeting structural, i.e., the load-bearing requirements, neglecting the importance of aerodynamic considerations. One of the main reasons for this approach is the lack of suitable development tools for creating aerodynamically efficient profiles for relatively *thick* geometries, such as the one investigated in this case. Consequently, undesired flow separations frequently occur within this region, resulting in unfavorable down-force and high drag instead of the desired lift and low resistance.

1.2. Known Airfoils Of Large Thickness

Figure 1 shows three earlier known aerodynamic airfoils, which mainly resulted from simple up-scaling of thickness from older, less thick (around 40%) ones. As can be immediately seen, a thin (<2% of chord) trailing edge (TE) is not at all appropriate, so profiles with a finite trailing edge (TE) are necessary. They were investigated early in [2]. Comparable profiles from the FX (Franz Xaver Wortmann) family were already used in the 1980s as for the GROWIAN 2 MW prototype [3]. As a final remark, it may be interesting to know of even earlier examples, for example, Hoerner in 1939 [4] (page 2–9) reported on measurements of a 70% thick strut in a water tunnel with pronounced region of negative lift slope.

Recently [5], a 60% profile (originally with a very thin TE) was investigated experimentally and by CFD, where, with the exception of one configuration, all geometries exhibited a negative c_L slope.

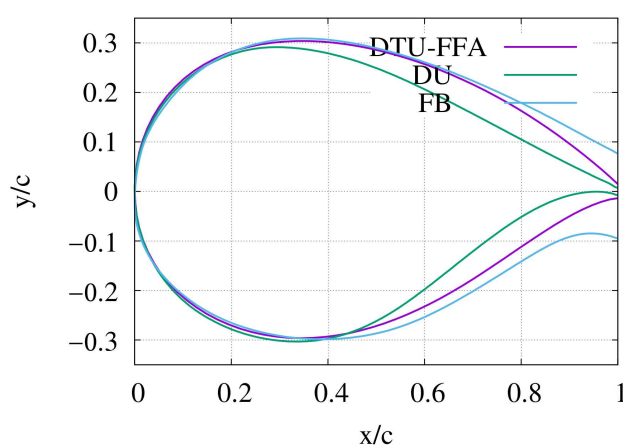


Figure 1. Earlier known profiles of 60% thickness.

1.3. Objectives

The objective of this research project is to develop a specific section within the transition area of the rotor blade with emphasis on the aerodynamic performance. However, it is important to mention that structural benefits result from reducing flow separation in the inner region and having a positive c_L slope. Therefore, both from the static as well as from dynamic loads and control schemes, additional benefits should result. More specifically, the aim is to examine a profile with a relative thickness of 60%, approximately between the last used profile (of 40% relative thickness) and a cylinder to avoid regions of negative lift and large drag. No design- c_L was defined; instead, a high positive c_l/c_D was aimed for.

The criteria and methodologies for designing such thick aerodynamic profiles are developed firstly. The main engineering problem to be overcome is to find a set of suitable geometric parameters which lead to a shape which fits structural and constraints for easy manufacturing and to avoid large drag and negative lift. Then, the most promising aerodynamic profiles are subjected to detailed numerical computational fluid dynamic (CFD) simulations, using approaches from simple panel codes to full 3D-RANS simulations. Subsequently, the profile exhibiting the most favorable properties is manufactured as a physical model and tested in a wind tunnel to validate its aerodynamic performance.

2. Methods

The standard methodology for designing a new aerodynamic profile is an iterative process, with a lot of flow simulation until a state is reached, ready for testing in a wind tunnel. For ideal flow (no viscous effects included, no turbulent flow within the boundary layer of the profile), a one-to-one correspondence exists between the local static pressure and the geometrical shape [6] so that an *inverse (design) mode* may then be possible. For real flow, no such mode is available; therefore, only direct flow simulation of a given shape is

possible. In the following, we use the term *CFD* for both models either using the panel or full RANS methods.

From the very beginning, an important constraint for the design process was that it could be easily transferred to industry, implying that especially only well-known computational codes should be used with one exception, the DLR tau code. Therefore—as an outcome of this discussion—our approach for designing a new profile consists of the following six steps, summarized in Table 1:

Table 1. Linear design approach.

1.	Investigate some known profiles of 60% thickness by CFD.
2.	Interpolate a circle and a typical profile of 40% thickness (AE60).
3.	Define an extended geometrical parameter space (BAL).
4.	Start from a specific 40% profile with increased TE-thickness (D60 series).
5.	Evaluate all shapes against implications due to manufacturability.
6.	Finally, select one profile for wind-tunnel testing.

For the choice of CFD code, a comparable rational applies. Well-known and easy-to-use panel code like Xfoil and MSES were demanded by our industrial partners. In a more sophisticated manner, RANS codes were used to check for a possible increase in numerical accuracy. Here, ANSYS fluent is state-of-the-art CFD code for industrial applications, and DLR tau is a more scientific code also for use in aerospace applications. The difference lies only in the modeling of laminar–turbulent transition [7]. One special point to be addressed from the beginning was to avoid both negative lift and a negative lift slope as observed in an investigation of a symmetrical, profile-like shape [8]. This unwanted behavior was confirmed by an initial analysis, in which a simple interpolated profile (see Figure 2) was investigated by CFD (see below), emphasizing the need for newly developed profiles.

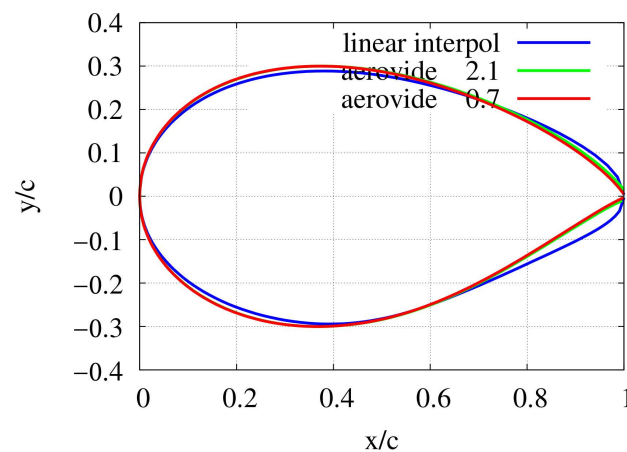


Figure 2. Geometric interpolations between a circle (at hub) and last profile (DU00-W2-401).

2.1. Geometric Interpolation between a Profile and a Circle

Typically, any wind turbine rotor blade has a circular flange, so there must be a transition from the last profile shape (in many cases, around 40% thickness by today) to a circle. The easiest way is to interpolate both shapes. Still, some freedom is present. Examples for different approaches are shown in Figure 2. However, this profile exhibits an unwanted negative lift at moderate AOA; see Figure 3. Figure 4 shows lift against drag.

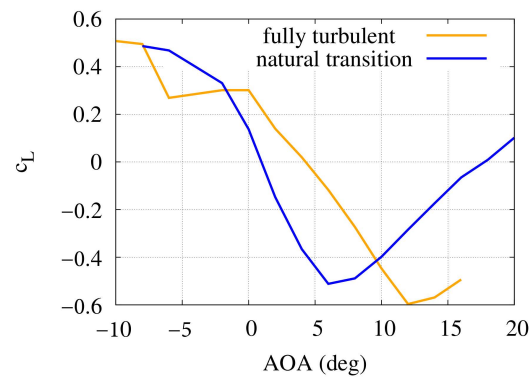


Figure 3. Negative lift for profile (aerovide 0.7) from Figure 2 at moderate AOAs.

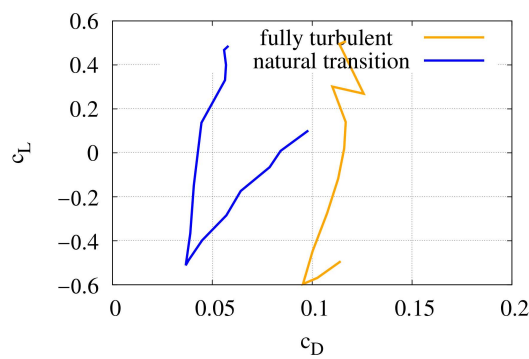


Figure 4. c_L vs. c_D (polar) for profile from Figure 2.

2.2. Geometric Design Inside an Increased Parameter Space

Using a slightly more advanced but still engineering approach, camber- and thickness-lines can be prescribed together with leading edge radius and trailing edge thickness, and are then transferred to a shape with continuous curvature. This was performed for nine shapes, abbreviated BAL001 to BAL009. Outline, lift, and drag curves of highest (c_l/c_D) BAL profile (BAL003) are shown in Figures 5–7. However, due to manufacturing restrictions (see Section 2.4), most of them had to be discarded. This approach was inspired by [9].

However, even these geometric shapes are not fully compatible with the chosen neighboring airfoil (DU00-W2-401) and cylinder. The demand for a better fit with regard to an easy manufacturing of the mold requires another approach; see Section 2.3.

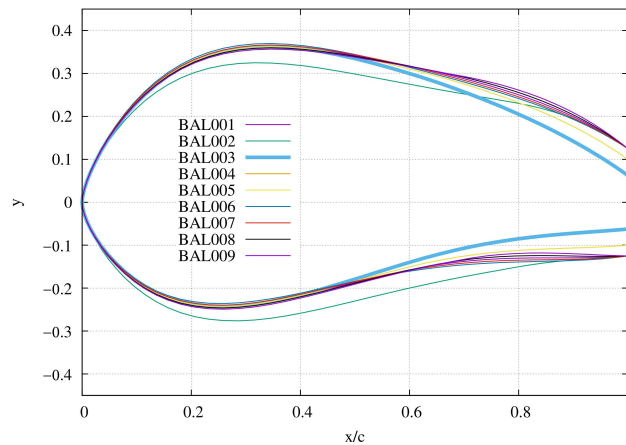


Figure 5. Outline of BAL-shapes. BAL003 emphasized.

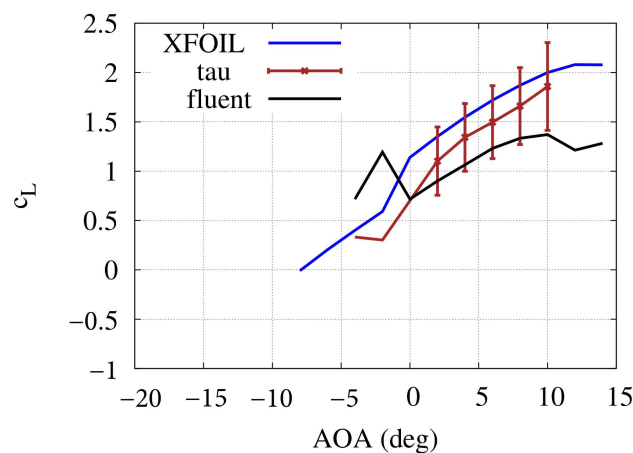


Figure 6. CFD for BAL003: c_L vs. AOA. Errors bars for tau calculation indicate amplitude of oscillation due to periodic vortex shedding.

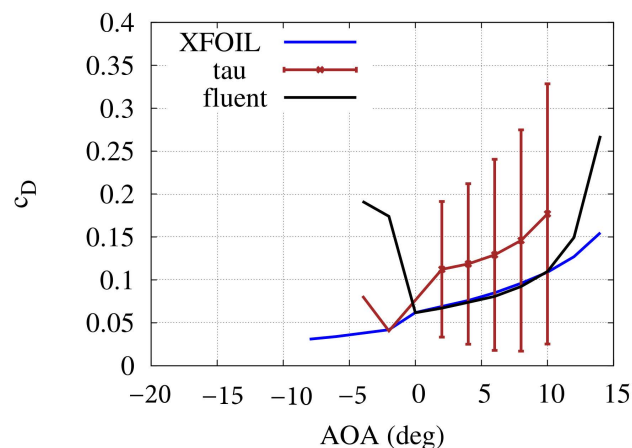


Figure 7. CFD for BAL003: c_D vs. AOA. Errors bars for tau calculation indicate amplitude of oscillation due to periodic vortex shedding.

2.3. Design Based on DU00-W2-401

Firstly, DU00-W2-401 was up-scaled with an increased relative thickness of 60% (D60A), and then the relative thickness of the flat-back was increased from 1% to 35% (D60B-V1). The geometry was changed to read for a smoother c_p (pressure) distribution (D60B-V2). Geometric compatibility (for easy manufacturing) was further improved by reducing the concave shape on the pressure side near the trailing edge (D60B-V3/V4). After some further iterations a preliminary geometry (D60B-V5) was developed and further investigated by 2D-RANS, see Section 3.2.

2.4. Implications Due to Manufacturability

Specific geometric compatibility is important for a 3D-blade to be manufactured in an economical way, especially when new profiles are inserted into the inner part, where usually the structural demands are essential. As this was considered to be handled with particular emphasis, we found the following to be important issues:

- No waviness and undulations;
- No winding of the separation line (of the mold);
- No discontinuities (gaps).

From known blade design experience of one of the project members, it can even be pointed out that the structural demands have higher priority than the aerodynamical properties. Nevertheless, there is a significant potential to increase turbine performance, which

has to be balanced against structural demands. Some of these geometrical constraints are as follows:

- Airfoil contour should fit well to the surrounding airfoil sections;
- Max thickness position between 0.25 chord length and 0.4 chord length;
- Smooth and round contour at LE and separation line (mold);
- Main structure (shear webs and spar caps) can be twisted inside the airfoil;
- Twist offset should have an insignificant effect on the structure;
- Angle of the flat-back adjustable (separation line);
- As much curvature as possible in the TE buckling fields.

As an important outcome of these constraints, it was decided to modify the trailing edge by tilting (see Figure 8). Figure 9 shows the resulting smooth course of the trailing edges of a generic 10 MW blade.

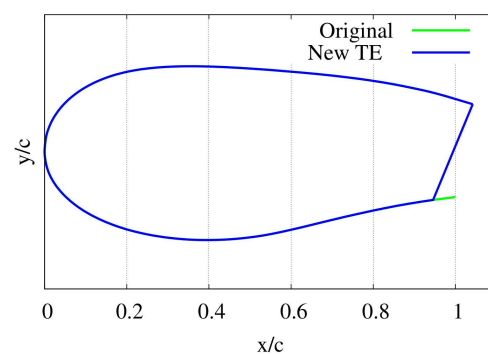


Figure 8. Proposed D60B-V5 airfoil for wind-tunnel testing. With and without tilted TE. Shape not to scale.

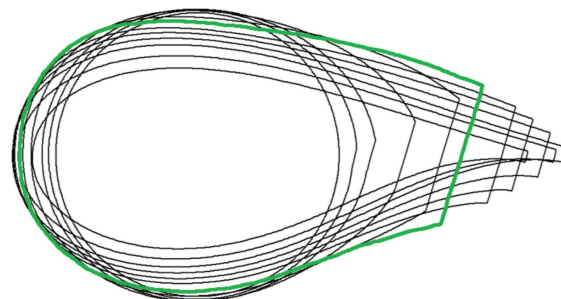


Figure 9. Smooth implementation of new profile with tilted TE (green) along a generic blade. Shape not to scale.

3. Numerical Investigations

3.1. Numerical Simulation I: Xfoil, MSES

First numerical simulations were conducted using tools such as Xfoil and/or MSES to preliminarily analyze and evaluate the performance of several 60% thickness airfoils developed for the targeted section within the transition area of the rotor blade. This allowed for quick iterations and optimizations of the developed profiles. It must be noted that even though these tools are not designed to be used on profiles with thick trailing edges or on thick profiles as those analyzed here, they are sufficient to provide initial feedback on the developed profiles within a limited range of accuracy.

Xfoil was developed by Mark Drela at MIT [10], and is widely recognized for its capability in airfoil analysis and design. To some extent, Xfoil was modified by van Rooij [11] to RFOIL. MSES [12], on the other hand, is a collection of programs for the analysis and design of single- or multi-element airfoils based on the Euler equations for predicting the aerodynamic behavior. Although a detailed documentation of equations

used is missing, it is known that viscous effects are included by integral boundary layer methods [13]. A recent review of *interacting boundary layer* methods is given in [14].

The objective at this step was a fast first assessment of the aerodynamic characteristics, particularly the lift and drag coefficients of the newly developed airfoil profiles. Based on the data obtained from the numerical simulations using Xfoil and MSES, plots illustrating the lift and drag characteristics of the developed airfoil profiles were generated. These plots serve as visual representations of the aerodynamic performance and provide a comparative analysis of the different airfoil designs. By examining the lift and drag data, the project aimed to identify the most promising airfoil profiles for further investigation and potential implementation in wind turbine blades.

3.2. Numerical Simulation II: 2D-RANS

In a subsequent stage, the selected airfoil profiles were subjected to further analysis using ANSYS fluent [15] and DLR tau [16] as more advanced and more accurate computational tools. Mesh sizes were 400 in circumferential direction and about 100 in the wall-normal direction. The computational domain was constructed as a circle of about 100 chords in diameter. In all 2D calculations, only two types of boundary conditions are necessary: wall (no slip) and far-field (this depends on the implementation, but in general a uniform velocity and static pressure is set.) A typical run took several hours on an HPC cluster. As the turbulence model, we used SST-k- ω enhanced by $RN_{\theta} - \gamma$ as the transitional model (ANSYS fluent) or e^N (DLR tau). The simulations were conducted in both steady and transient conditions primarily for a chord-based Reynolds number of 2 M. The profile chosen for manufacture and a subsequent wind tunnel test was also evaluated at a chord-based Reynolds number of 2.7 M. No grid independence studies were performed, as no exact knowledge of accuracy was necessary.

The resulting lift, drag, and moment data provided insights into the aerodynamic performance of the profiles, enabling a comprehensive evaluation of their suitability for practical implementation in wind turbine blades. It is important to note that the RANS simulations facilitated a more realistic representation of the flow than Xfoil or MSES but still depended on additional modeling, for example, for the prediction of a transition location and turbulent regions in general.

The data obtained from these simulations formed a basis for the selection of the profiles to be tested in the wind tunnel. The lift and drag characteristics provided insights into the performance of the profiles under varying flow conditions, aiding in the quantification of the range of aerodynamic forces expected during measurement in the wind tunnel.

3.3. Numerical Simulation III: 3D-RANS

Finally, 3D-RANS (ANSYS fluent) was used to investigate possible deviation from 2D behavior. A 120°-segment with periodic boundary conditions was chosen as the computational domain. The inlet was 5 rotor diameters in front of, and the outlet 10 rotor diameters behind, the rotor plane. The mesh around the blade used partial structured meshes, whereas a background mesh was made from tets. In total, the mesh size was 25 M cells. Apart from the wall-type boundary condition on the blade, the remaining five outer surfaces consisted of two periodic types, one inflow and one pressure outlet (far-field). The remaining shroud of the cylinder was either set to pressure outlet or symmetry depending on the degree of convergence to be reached. Typically, tens of thousands iterations have to be performed until mass residuals decrease to three or more orders of magnitude.

Very recently, an open-access design of a 22 MW, 282 m rotor diameter, off-shore machine was released [17], in line with older 5 MW and 10 MW versions. However, we used our own design, more suited for specific use in state-of-the-art commercial wind turbines. The very different design is obvious in Figures 10 and 11.

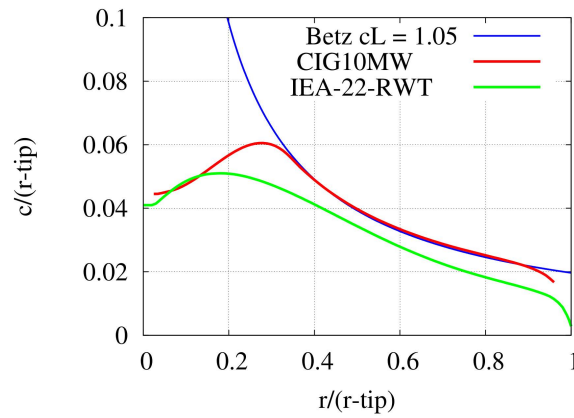


Figure 10. Chord distribution of CIG10MW and IEA-22MW reference wind turbine.

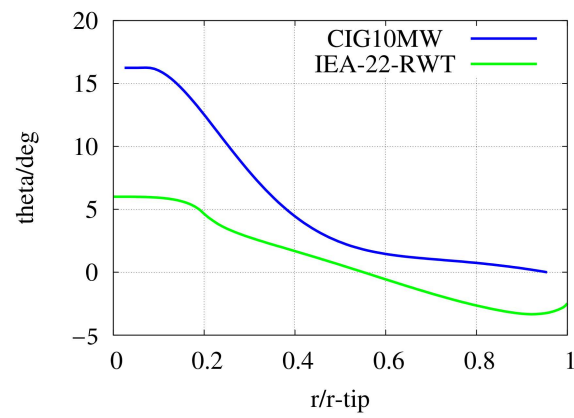


Figure 11. Twist distribution of CIG10MW and IEA-22MW reference wind turbine.

The new profile is located at a spanwise radius of $x_m = 17$ m as seen in Figure 12. In addition, Figure 13 shows the complete set of polars. Different 3D meshes (up to a size of 25 M cells) were prepared pointwise, but no mesh-independence study was performed because the 3D effects (due to rotation) were investigated only qualitatively.

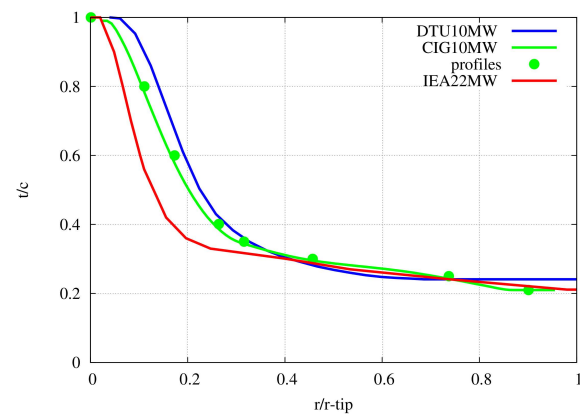


Figure 12. Location of newly developed $t/c = 0.6$ profile for generic CIG10MW blade, radius (r) in m, and thickness as t/c . KSS is the name of our BEM Code. Rotor diameter = 100 m. Compared to IEA-22 MW reference wind turbine [17].

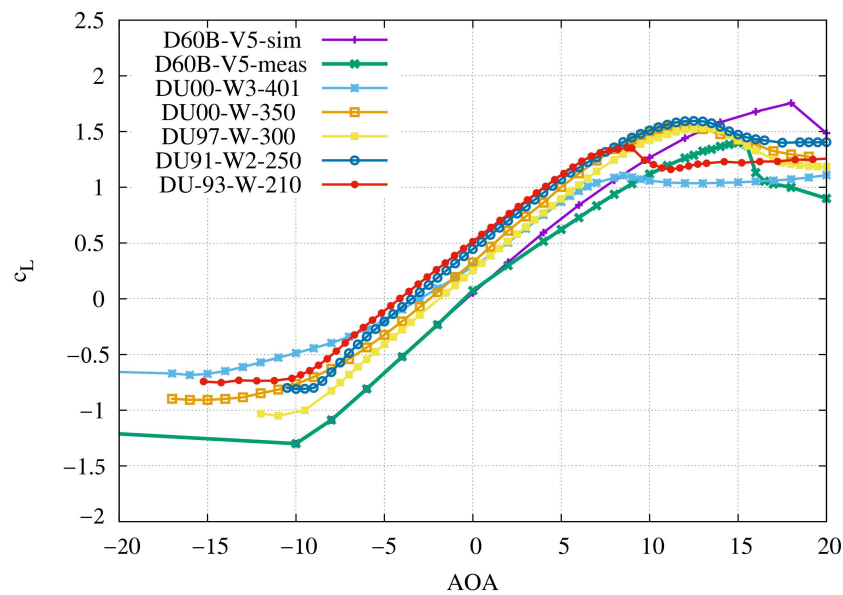


Figure 13. Complete set of polars (c_L vs. AOA) for CIG10MW blade. D60B-V5 is presented with simulated and measured data, see Table 2.

Table 2. Comparison of maximum power coefficient (cP_{max}) improvement when using various profiles of large (57% to 60% relative thickness). It should be noted that various BEM codes were used, including an in-house code, among others.

Case	cP_{max}	ΔcP in %
AE60 (spline)	0.468	
AE60 (linear)	0.476	1.7
W570	0.480	2.5
BAL003	0.486	3.8
D60B-V5 (BEM)	0.485	3.6
D60B-V5 (CFD)	0.490	4.7

4. Measurement Set-Up

The wind tunnel is of the closed-circuit type, and can be operated either with an open (OTS) or a closed (CTS) test section. The closed test section is possible due to the use of a second nozzle and a modular test section system. For 2D airfoil tests, the wind tunnel is operated with a rectangular $2.75 \text{ m} \times 1.25 \text{ m} \times 5 \text{ m}$ ($W \times H \times L$) closed test section. The use of wall pressure (WP) measurements, airfoil surface pressure (PP) measurements, force balances (FBs), and a wake rake (WR) provides the necessary equipment for aerodynamic airfoil characterization. Wind tunnel calibration including standard correction methods are described in [18,19]. Static surface pressure was measured by *HTD series digital differential pressure sensors* from FirstSensor[®], and data were obtained by a *CompaqDAQ-Module* from National Instruments. The sampling rate was 10 Hz and integration time (for each AOA) was 25 secs. The thermographic equipment consists of a ImageIR[®] 8300 by INFRATEC. As the tunnel-entry run took one week (five working days), the reproducibility could be checked each day by using the clean model. A more complete and detailed description is given in [19]. Figure 14 shows the airfoil model mounted in the wind tunnel.



Figure 14. Experimental set-up.

5. Results

5.1. Wind Tunnel Measurements

To validate the performance and design parameters of the D60B-V5 airfoil, measurements were conducted at Deutsche WindGuard's aeroacoustic wind tunnel (DWAA) in Bremerhaven, Germany. For airfoil testing, the DWAA wind tunnel operates a $1.25\text{ m} \times 2.7\text{ m} \times 5\text{ m}$ closed test section, achieving Reynolds numbers up to 6×10^6 , with flow speeds up to 100 m/s at turbulence level of $\leq 0.05\%$.

The 2D model, manufactured in carbon fiber by Glasfaser Flugzeug-Service GmbH, has a chord length of 0.5 m , a relative thickness of 60% , and spans the entire test section height of 1.25 m . To investigate the airfoil surface pressure, a total of 94 pressure taps were installed chordwise, with an appropriate spanwise offset. The "NEW TE" geometry was achieved by a means of an exchangeable trailing edge. The airfoil model was mounted vertically, with its rotational axis at $x/c = 1/4$. The (shape factor) Λ -value used for the AGARD-corrections was 1.825 [18–20].

In total, data from 34 polars (a selected number is described in Table 3) were measured, including several *more or less standard aerodynamic devices* like vortex generators, zig-zag tape and gurney flaps. In addition, due to the special requirements of the project, a tilted TE (for smoother fitting into the blade mold) and a splitter plate (for reducing pressure drag) were investigated. Zig-zag tape was placed at $x/c = 0.05$ on the suction side and $x/c = 0.1$ on the pressure side. The location of the gurney flap was mounted on the pressure side of the trailing edge. Configurations VG1, VG2, and VG3 refer to their locations on the upper (suction) side.

The main effect of zig-zag tape (POL 13) is to generate a fully turbulent flow but results in more drag and less lift only. Gurney flaps (POLs 73 and 85) give rise to much more lift

(cL_{max} rises from 1.55 (clean) to 2.1), but drag is also increasing so that in total, no increase in L2D is visible. Surprisingly, the splitter plate (POLs 85, 88 and 91) reduces drag (cD_{min}) from about 0.09 down to 0.05. We performed RANS simulations to look at the mechanism which lies behind this effect. Clearly, the change in surface pressure at the flat back must be responsible for this decrease. Unfortunately, due to a lack of a turbulence model to describe the flow separation from sharp corners accurately enough, a clear explanation cannot be given within this study. As a further important observation, it can be seen that all polars show real airfoil behavior (more lift than drag and positive cl -slope), despite the profile's exceedingly high thickness. An explanation may lie in the observation that the flow behind the very thick TE extends the *effective* chord to much larger values, see Figures 15 and 16.

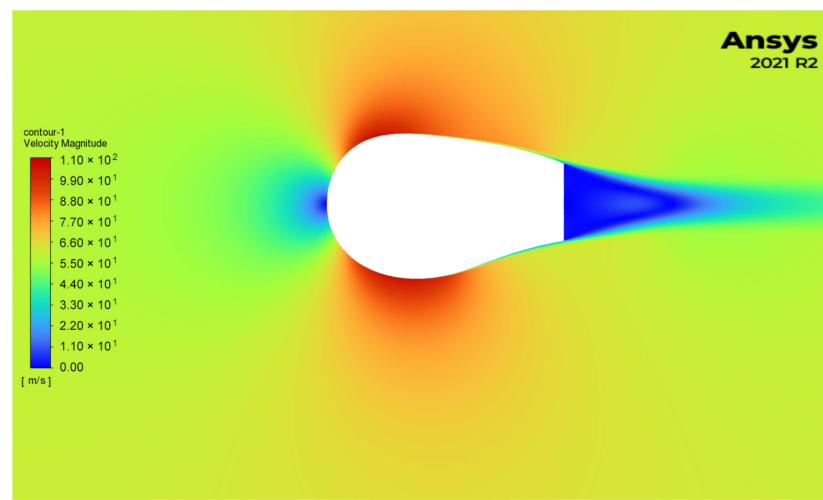


Figure 15. Sample velocity field at 0° AOA, simulated with ANSYS fluent.

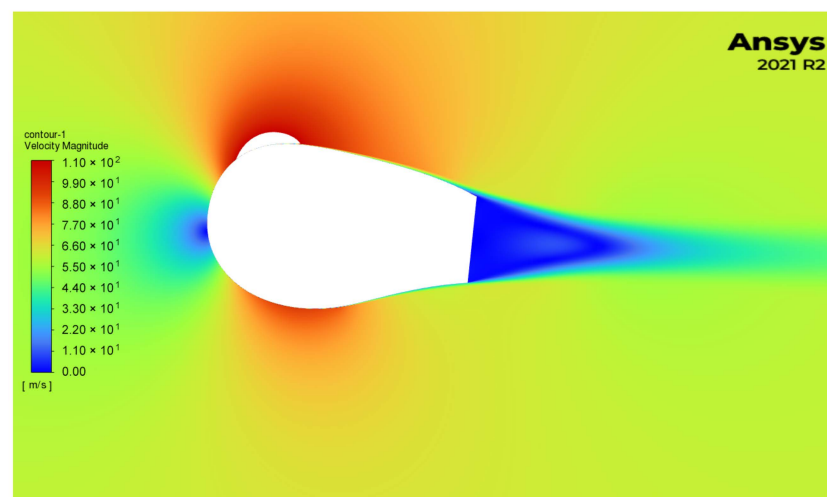


Figure 16. Sample velocity field at 6° AOA, simulated with ANSYS fluent.

Most instructive is a comparison of measurements against simulation. Examples of measured and simulated pressure coefficients are shown in Figures 17 and 18. There are some deviations visible (especially on the lower side in Figure 16), but no clear explanation could be found. Global values c_L , c_D are seen in Figure 19.

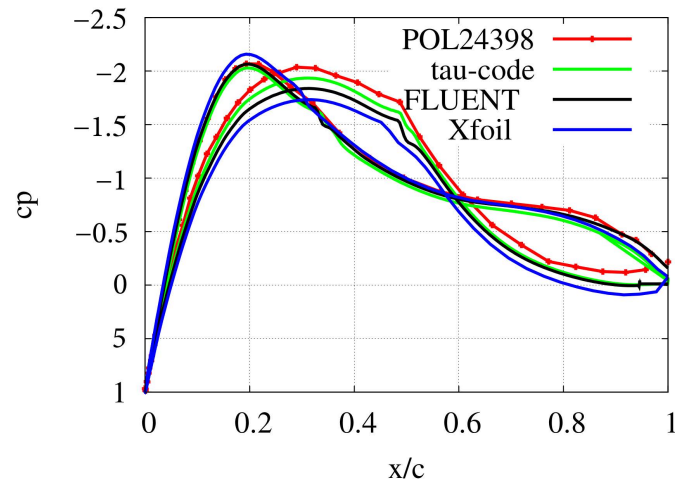


Figure 17. Pressure (coefficient) of clean configuration at 0° AOA. Results from panel code Xfoil and RANS codes ANSYS fluent and DLR tau.

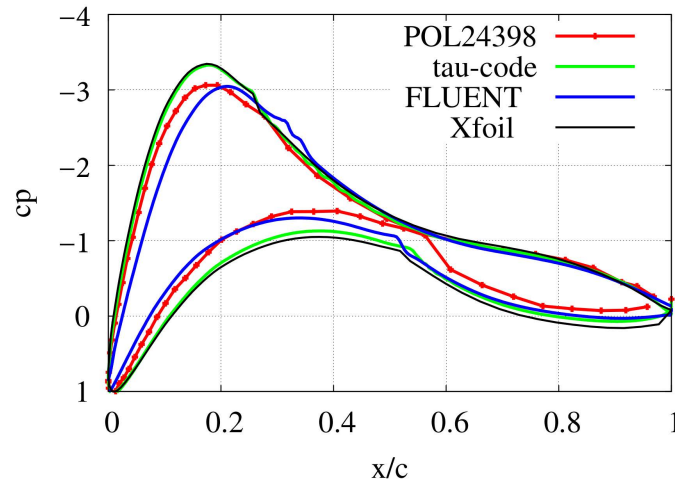


Figure 18. Pressure (coefficient) of clean configuration at 6° AOA Results from panel code Xfoil and RANS codes ANSYS-fluent and DLR-tau.

Drag could be reduced by almost a factor of 2 (down to $c_{D-min} \approx 0.05$), which corresponds to a notable reduction in under-pressure at the TE by using a splitter plate.

Table 3. Explanation for selected polars from Figure 20. First 3 digits omitted.

Number	RN/10 ⁶	Remark
13	2.75	Zigzag tape 0.125 mm
18	2.75	as 13
25	2.75	clean
45	2.75	VG2
73	2.75	GF 8 mm on PS
85	2.75	GF and splitter plate
88	2.75	VG2 and splitter plate
91	2.75	Splitter plate

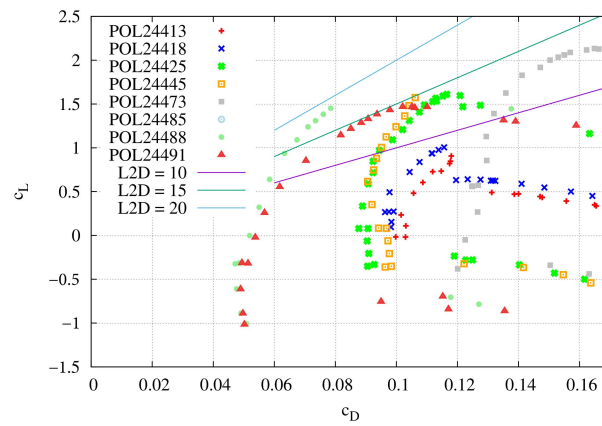


Figure 19. Drag reduction by using a splitter plate; 2D-CFD results for clean case included.

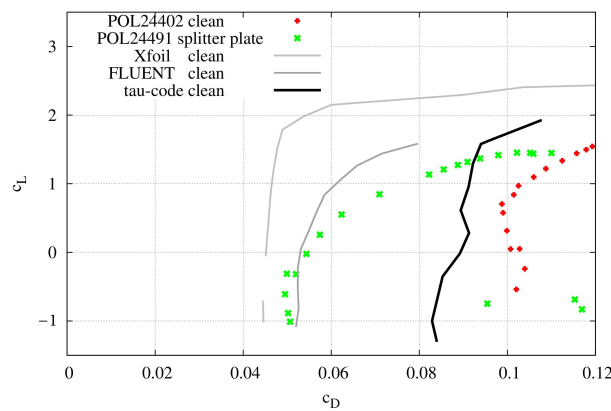


Figure 20. Selected measured polars, description of configuration is shown in Table 3.

5.2. Numerical Investigation of Possible 3D-Effects

Airfoil D60B-V5 was implemented into a generic 10 MW wind turbine rotor blade (rotor diameter: 200 m) for use in 3D-RANS (ANSYS fluent) calculations, see Section 3.3.

As the new profile operates in the very inner part, 3D effects are to be expected. Figure 21 shows a comparison of sectional tangential forces at rated conditions. It can be seen that for $r < 30$ m, BEM and 3D-CFD show rather different results: much more positive tangential forces resulting in more power are visible. Compared to global c_p -values, CFD gives 0.490 ± 0.001 , almost equal to the value from BEM (0.485).

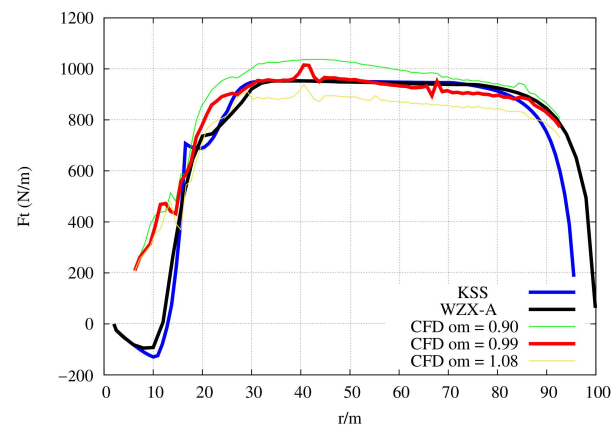


Figure 21. Comparison of radial distribution of tangential (driving) forces. BEM (KSS and WZX-A) vs. 3D-RANS. Especially in the part from where the 60% profile ($r < 17$ m) starts, pronounced (positive) changes are visible. $\omega = \omega$ is the angular velocity.

An important task—possible to be checked in 3D-RANS only—is to test if the angle of attack is not changed by 3D effects. To estimate, a so-called *inverse-BEM* method was applied [21], which is known not to be the most accurate but by far the easiest and most efficient to implement. A typical set of data for rated conditions (TSR = 9.5, pitch = 0°) is presented in Table 4. The 3D-CFD gives higher induction but a somewhat lower AOA and higher c_L .

Efficiencies predicted by BEM (5 profiles) and/or CFD (only one profile D60B-V5) are listed in Table 2.

An improvement in terms of c_P of $4.2\% \pm 0.6\%$ is predicted from all simulations.

Table 4. Extracted 3D-airfoil data by using invBEM at $\omega = 0.99$ and $v_{wind} = 11$ m/s at $r = 20$ m.

Case	AOA	c_L	c_D	a
BEM(KSS)	7.0	1.00	0.045	0.34
fluent	6.1	1.10	0.038	0.42

6. Discussion

As the design targets were not formulated in much detail, apart from having positive lift slope and low drag, our methodology seems to be effective, as it is able to satisfy a large set on geometric constraints.

Regarding numerical evaluation, Xfoil and MSES tend to over-predict lift on one side, while on the other side they under-predict drag. Estimating c_L^{max} and c_D^{min} seems not to be possible with reasonable accuracy (let us say 1%). In addition, in some cases, it was not possible to receive a converged solution when using MSES.

The 2D-RANS incorporates more details from flow physics without too much fitting as in the mentioned methods above. A major drawback is that there is much more effort to be spent in the model preparation. This applies to mesh preparation in particular and becomes important when more variations have to be investigated. Due to the pronounced thickness of the TE, the flow field seems to be unstable, making transient simulations necessary. As a result, strong oscillations (see Figures 22 and 23) occur. The corresponding amount of variations in numbers is indicated by *error-bars*.

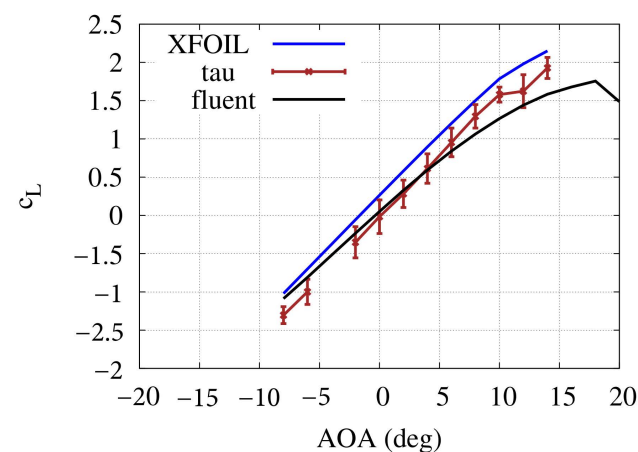


Figure 22. Comparison of simulated 2D polar from three codes (Xfoil, fluent, and tau) for the final design: c_L vs. AOA.

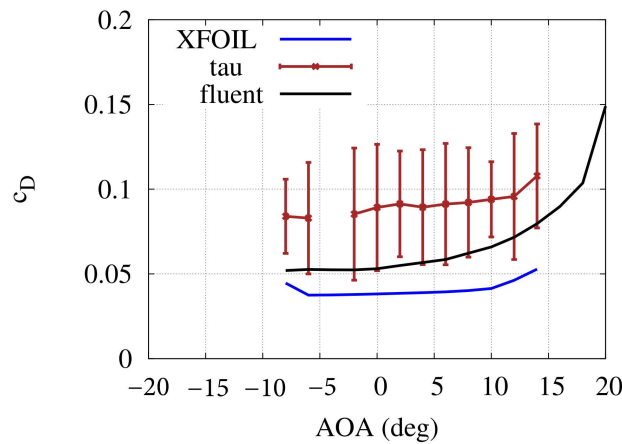


Figure 23. Comparison of simulated 2D polars from three codes applied for the final design: c_D vs. AOA.

The 3D-RANS is necessary to assess 3D effects, which are important in the most inner part with large c/r (local chord against local distance from rotational center). When applied to a specific test turbine blade, the Reynolds number is much larger (5 M instead of 2.7 M as in the wind tunnel test) for our numerical 3D set-up. As in the wind-tunnel test, RN was increased from 1 M to 2.7 M, see Figure 24, we do not expect adverse effects for higher RN.

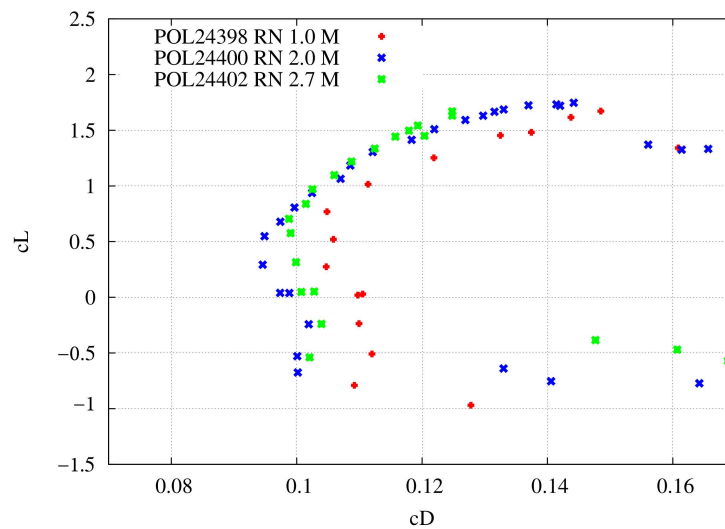


Figure 24. RN variation for clean airfoil D60B-V5 measured in DWAA.

As a general remark, it has to be mentioned that predicting drag (reduction) still is a challenge for RANS and depends heavily on the turbulence and transition model. Changing, for example, from SST- $k-\omega$ (state-of-the-art) to $k-\epsilon$ (outdated) may alter drag prediction in the order of 5%.

A 2D wind-tunnel model was tested in a wind tunnel at Reynolds numbers up to 2.7 million. Vortex generators, gurney flaps, and zig-zag tape were used to test the degree to which the aerodynamic properties could be influenced. Wind tunnel corrections [19] may be stressed by high thickness and/or high blockage but proved to be reliable.

As one of the most remarkable findings, a strong decrease in drag was observed when using a specific splitter plate. We attribute this to the reduction in under-pressure at the trailing edge.

7. Summary and Conclusions

A 60% thick airfoil for use in the root region of a wind turbine blade has been developed by using a variety of approaches, including pure geometrical construction by providing a few characteristic quantities (like the location of the maximum thickness, the shape of the camber line, the TE thickness, etc.). Four different CFD codes (Xfoil, MSES, ANSYS fluent and DLR tau code) were used to select two base shapes to be investigated in the DWAA wind tunnel at Reynolds Numbers up to 2.75 million. Several configurations (clean, VG, GF, and zig-zag tape) were used. TE inclination was adapted for smoother variation in a blade mold, and a splitter plate was additionally placed at the TE with the remarkable result of decreasing C_D^{min} down to ≈ 0.05 . A generic blade for a 10 MW turbine was defined (CIG10MW), and it could be shown that using the newly developed profile (named D60B-V5) may lead to an increase in c_p^{max} in the range of 4%, which is a very high value. We embedded the new profile into a generic aerovide blade (AE4.3–78.7) to be used in a 4.3 MW wind turbine. Performance as a function of mass increase was investigated. A similar—although not as high as mentioned above—increase in $c_{p,max}$ resulted but with a comparably smaller increase in c_T and mass. No indications of adverse 3D effects were observed. All results (from simulation as well as from measurement) seem to be consistent in the sense that the linear design approach (AE60 → BAL003 → D60B_V5) has led to a shape that exhibits the expected aerodynamic behavior of having positive lift slope and low (e.g., <0.1) drag, leading to L2D above 10. Using a combination of a tilted TE and a splitter plate, a novel airfoil design results.

Author Contributions: Conceptualization, A.P.S.; methodology, A.P.S., V.K. and N.B.; software, B.A.L. and Z.W.; validation, A.P.S. and N.B.; formal analysis, all; investigation, all; resources, A.P.S. and N.B.; data curation, J.S.; writing—original draft preparation, B.A.L. and A.P.S.; writing—review and editing, N.B.; visualization, B.A.L., Z.W. and A.P.S.; supervision, A.P.S.; project administration, A.P.S. and B.A.L.; funding acquisition, A.P.S. All authors have read and agreed to the published version of the manuscript.

Funding: Funding by Deutsche Bundesstiftung Umwelt (DBU), Germany, under contract number 37253/01-24/0 is gratefully acknowledged.

Institutional Review Board Statement: Not applicable.

Informed Consent Statement: Not applicable.

Data Availability Statement: Part of the data presented in this study are available upon request from the corresponding author.

Acknowledgments: Special thanks go to Dirk Schötz for his constant and efficient support during many projects over the years. We also thank two unknown referees in an earlier version for useful hints. Usage of HPC resources provided by the North-German Supercomputing Alliance (then: HLRN, now: NHR) are gratefully acknowledged.

Conflicts of Interest: Nicholas Balaesque and Janick Suhr work at Deutsche WindGuard Engineering GmbH and declare no conflict of interests. Volker Kremer works in AEROVIDE GmbH and declare no conflict of interests.

Abbreviations

The following abbreviations are used in this manuscript:

AOA	Angle Of Attack (α)
AE60	profile shape by simple interpolation
BAL	Brandon Arthur Lobo
CFD	Computational Fluid Dynamics
CIG	China–India–Germany
DLR	German Aero-Space Association
DNW	Deutsch-Niederländische Windkanäle - German-Dutch Wind Tunnels
drag counts	$10^4 \cdot c_D$

DTU	Danish Technical University
DU	Delft University, The Netherlands
DWAA	Deutsche WindGuard aeroacoustic Wind Tunnel
DWGE	Deutsche WindGuard Engineering GmbH
FFA	Flygtekniska försöksanstalten, Sweden
HLRN	HochLeistungsRechenzentrum Nord
HPC	High Performance Cluster
IEA	International Energy Agency
lift-to-drag	Lift-to-Drag Ratio c_L/c_D
L2D	Lift-to-Drag Ratio
KSS	Korjahn Schlipf Schaffarczyk, name of BEM code
M	million
POL	polar
NHR	Nationales Hochleistungsrechnen
RANS(E)	Reynolds Averaged Navier Stokes (Equations)
RN	Reynolds Number
RWT	Reference Wind Turbine
TE	Trailing Edge
TSR	Tip-Speed Ratio (λ)
c_D	Drag coefficient
c_L	Lift coefficient
c_p	Pressure coefficient
c_P	Power coefficient
Λ	Geometric shape factor used for wind tunnel correction [19]

References

- Schaffarczyk, A.P. *Introduction to Wind Turbine Aerodynamics*, 3rd ed.; Springer: Heidelberg, Germany, 2024.
- Standish, K.; van Dam, C. Analysis of Blunt Trailing Edge Airfoils. In *Proceedings of the 41st Aerospace Sciences Meeting and Exhibit, Reno, NV, USA, 6–9 January 2003*; AIAA: Reston, VA, USA, 2003; Chapter 6, p. 353. [CrossRef]
- Althaus, D.; Wortmann, F.X. *Stuttgarter Profilkatalog 1: Meßergebnisse aus dem Laminarwindkanal des Instituts für Aerodynamik und Gasdynamik der Universität Stuttgart*; Vieweg: Braunschweig, Germany, 1981.
- Hoerner, S. *Fluid-Dynamic Lift*, 2nd ed.; Liselotte, A.H., Ed.; Cambridge University Press: Cambridge, UK, 1985.
- Pei, Z.; Xu, H.Y.; Deng, L.; Li, L.X. Influence of the Blunt Trailing-Edge Thickness on the Aerodynamic Characteristics of the Very Thick Airfoil. *Wind* **2023**, *3*, 439–458. [CrossRef]
- Eppler, R. *Airfoil Design and Data*; Springer: Berlin/Heidelberg, Germany, 1990.
- Özlem, C.Y.; Pires, O.; Munduate, X.; Sørensen, N.; Reichstein, T.; Schaffarczyk, A.P.; Diakakis, K.; Papadakis, G.; Daniele, E.; Schwarz, M.; Lutz, T.; Prieto, R. Summary of the Blind Test Campaign to predict High Reynolds number performance of DU00-W-210 airfoil. In *Proceedings of the 35th Wind Energy Symposium, Grapevine, TX, USA, 9–13 January 2017*. [CrossRef]
- Schaffarczyk, A.P.; Arakawa, C. A thick aerodynamic profile with regions of negative lift slope and possible implications on profiles for wind turbine blades. *Wind Energy* **2021**, *24*, 162–173. [CrossRef]
- Rochholz, H. *A New Airfoil Family for Rotor Blades*; Technical Report (Confidential), Leitwind. Available online: <https://dspace-erf.nlr.nl/server/api/core/bitstreams/d29bb7e6-b290-480d-9687-17841973c3bc/content> (accessed on 14 June 2024).
- Drela, M. XFOIL: An Analysis and Design System for Low Reynolds Number Airfoils. In *Lecture Notes in Engineering*; Springer: Berlin/Heidelberg, Germany, 1989; pp. 1–12.
- van Rooji, R. *Modification of the Boundary Layer Calculation in RFOIL for Improved Airfoil Stall Prediction*. Technical Report, IW-96087R; Delft University of Technology: Delft, The Netherlands, 1996.
- Drela, M. *A User's Guide to MSES 3.05*; Massachusetts Institute of Technology (MIT): Cambridge, MA, USA, 2007.
- Drela, M. *Flight Vehicle Aerodynamics*; The MIT Press: Cambridge, MA, USA, 2014.
- Özdemir, H. Interacting Boundary Layer Methods and Applications. In *Handbook of Wind Energy Aerodynamics*; Springer International Publishing: Berlin/Heidelberg, Germany, 2022; pp. 253–302. [CrossRef]
- ANSYS *Fluent Tutorial Guide*. 2020. Available online: <http://s2.bitdl.ir/Engineering/ALL.ANSYS/ANSYS%2012%20DOCUMENTATION/Fluent/fludf.pdf> (accessed on 14 June 2024).
- Krimmelbein, N.; Radespiel, R. Transition prediction for three-dimensional flows using parallel computation. *Comput. Fluids* **2009**, *38*, 121–136. [CrossRef]
- Zahle, F.; Barlas, A.; Lønbaek, K.; Bortolotti, P.; Zalkind, D.; Wang, L.; Labuschagne, C.; Sethuraman, L.; Barter, G. *Definition of the IEA Wind 22-Megawatt Offshore Reference Wind Turbine*; DTU Wind Energy Report E-0243 IEA Wind TCP Task 55; Technical University of Denmark: Lyngby, Denmark, 2024. [CrossRef]
- Ewald, B.F.R. *Wind Tunnel Wall Corrections*; Technical Report AGARD-AR-336, Advisory Group for Aerospace Research & Development; North Atlantic Treaty Organization: Brussels, Belgium, 1998.

19. DWGE GmbH. *Deutsche WindGuard's Aeroacoustic Wind Tunnel*; Technical Report DWGE_WT_TD_1; Deutsche WindGuard Engineering GmbH: Varel, Germany, 2021.
20. Fluid Dynamics Panel Working Group 15. *Quality Assessment for Wind Tunnel Testing*; Technical Report AGARD-AR-304, Advisory Group for Aerospace Research & Development; North Atlantic Treaty Organization: Brussels, Belgium, 1999.
21. Lindenburg, K. *Investigation into Rotor Blade Aerodynamics*; Technical Report, ECN-C-03-025; Kimerius Aircraft: Barcelona, Spain, 2003.

Disclaimer/Publisher's Note: The statements, opinions and data contained in all publications are solely those of the individual author(s) and contributor(s) and not of MDPI and/or the editor(s). MDPI and/or the editor(s) disclaim responsibility for any injury to people or property resulting from any ideas, methods, instructions or products referred to in the content.